Catalysis Today 157 (2010) 440–445

Contents lists available at ScienceDirect

Catalysis Today

journal homepage: www.elsevier.com/locate/cattod

Catalytic combustion of CH_4 and H_2 into micro-monoliths

Stefano Tacchino, Luigi D. Vella, Stefania Specchia*

Department of Materials Science and Chemical Engineering, Politecnico di Torino – Corso Duca degli Abruzzi 24, 10129 Torino, Italy

ARTICLE INFO

Article history:
Available online 3 April 2010

Keywords:
Catalytic combustion
Methane–hydrogen mixtures
Pd/Pt-based catalysts
Monolith
Microreactor

ABSTRACT

Catalytic combustion of CH_4 or other gaseous HCs in microscale channels is becoming the key technology for various portable power generation devices that could replace current batteries to meet the increasing demand for more efficient, longer lasting and more environmentally friendly energy-consuming utilizations. New type of catalysts for the CH_4/H_2/air lean mixtures oxidation in drastic conditions were proposed and investigated; they were lined on SiC monoliths (dimensions 6 mm × 6 mm × 22 mm) and tested into a lab-microreactor able to reach high power density ($7.6\,MW_{th}\,m^{-3}$). The catalysts were directly deposited on the monoliths via in situ solution combustion synthesis. The most interesting performance on the oxidation of CH_4/H_2/air lean mixtures was obtained with the monolith 2% Pt/(5% Al_2O_3), 2% Pd/(5% $NiCrO_4$), followed by 2% Pd/(5% $CeO_2{\cdot}ZrO_2$) and 2% Pd/(5% $LaMnO_3{\cdot}ZrO_2$); the monolith 2% Pt/(5% Al_2O_3) behave better by burning CH_4 or H_2 alone. For the Pd-based catalysts, the addition of H_2 to the reactive mixture led to an improvement of the CH_4 combustion, whereas this did not happen for the Pt-based one. The addition of H_2 to the gas mixture allowed to a decrease of the CH_4-T_{50} and CH_4-T_{100} compared to the combustion of CH_4 alone, and the conversion curves slope becomes steeper: the higher the H_2 concentration, the higher the mixture reactivity towards CH_4 oxidation, probably due to the larger production of H_2 reactive radicals ($OH^\bullet$).

1. Introduction

The catalytic combustion of hydrocarbons (HCs) is nowadays the subject of considerable interest in view of its several prospective both as industrial and domestic applications [1–3], with attention focused on developing new processes aimed to limit air pollution [4]. The use of a catalyst, in fact, promotes the full and efficient oxidation of HCs at temperatures far lower than those established in typical flames, with high combustion efficiency [3]. As a consequence, CO and unburned fuel emissions are drastically reduced with respect to non-catalytic systems. Moreover, also the noxious emission of NO_x are decreased, thanks to the lower combustion temperatures at which thermal-NO_x formation becomes limited [4,5]. Catalytic combustion enables, additionally, the burn-out of air/fuel mixtures well outside their flammability region, and this is a desirable feature for safer domestic applications or for energy recovery from diluted HCs streams (volatile organic compound combustion [4]).

Methane is the most stable hydrocarbon and hard to be oxidized since it is characterized by the strongest C–H bond of all paraffins [6,7]. It is also a powerful greenhouse gas, with a global warming potential higher than that of CO_2 at equivalent emissions rate [8]. Mixing CH_4 with CO, H_2 or light HCs, might be advantageous due to the higher oxidation reactivity of the latter which could facilitate the burning appliances start-up [9] and/or stabilise the catalytic reaction without the need of further preheating [10]. CH_4/H_2 mixtures are of great interest nowadays: it is worldwide known that the fuel called Hythane® [11], i.e., a blend of 5–20% of H_2 in CH_4, is becoming an alternative fuel to power CNG vehicles with the clear advantage of lower CO_2, CO and NO_x emissions. The higher the H_2 content, the lower the noxious emissions and the higher the calorific value of the mixture when compared with CNG vehicles. Depending upon the blend, many of the vehicles currently running on CNG will not introduce any modifications to run on Hythane®. Moreover, Hythane® can be easily integrated into the existing CNG infrastructure, making it simply and rapidly exploitable in practical applications, not only related to vehicles mobility [12,13], as proved also by many research and demonstration projects in Europe, America and Asia [14–16], but also for portable applications [17–20].

Supported noble metal-based catalysts, especially PdO and Pt, exhibit an outstanding activity for CH_4 combustion, but are particularly sensitive to operation at elevated temperatures larger than about 850 °C [21,22]. PdO loses its activity mainly due to its decomposition to Pd [3], while Pt suffers from sintering and volatilization [21–23]. In particular, the active state of Pd particles is a fully oxidized surface state, and the formation of oxygen species on the surface of PdO is crucial to explain the catalytic activity [24,25]. On

---

* Corresponding author. Tel.: +39 011 0904608; fax: +39 011 0904699.
E-mail address: stefania.specchia@polito.it (S. Specchia).

0920-5861/$ – see front matter © 2010 Elsevier B.V. All rights reserved.
doi:10.1016/j.cattod.2010.03.002

the contrary, referring to CH_4 combustion over Pt, a less oxidized Pt surface seems to be more active compared to a more oxidized one [8,26,27].

Combustion in micro- and meso-scale channels is becoming the key technology for various portable and remote power generation devices that could replace current batteries to meet the increasing demand for more efficient, longer lasting and more environmentally friendly operation in various civil and military devices for electronic and telecommunication applications [19,20,28,29]. Although combustors are not power generators by themselves, they can be used in conjunction with other devices (thermoelectric, piezoelectric, inert fluid cycles, etc.) to produce electrical power. In particular, in the recent years some combustors have been applied to energize thermoelectric systems to produce electrical power, although with low overall efficiency [28,30,31]. A miniaturized combustion device with only a mere 3% system efficiency, in fact, would compete with top batteries simply from the fact that the fuel is easily rechargeable. HCs have an energy density significantly higher than that of the traditional Li batteries (up to $40\,\mathrm{MJ\,kg^{-1}}$ vs. $1.2\,\mathrm{MJ\,kg^{-1}}$) that are currently used in laptops, cellular phones, and other portable electronics devices [29]. Recent works showed that it is possible to sustain homogeneous flames in submillimeter channels in specially constructed ceramic micro-burners [32–34]. The wall thermal conductivity plays an important role in the flame stability and materials integrity of micro-burners [33]: low wall thermal conductivity limits the upstream heat transfer through the wall, which limits the preheating of the feeding and causes blowout; on the contrary, high wall thermal conductivity allows lower wall temperatures, which is favourable to limit the NO_x formation but could cause extinction. Therefore, submillimeter scale catalytic combustion results in turns particularly interesting.

The aim of the present work deals with the investigation of new type of catalysts, lined on SiC monoliths, for the CH_4/H_2/air lean mixtures oxidation. The catalytic monoliths were specifically designed to be inserted in a thermoelectric micro-device, for portable or remote power generation. Anyway, the coupling of the micro-combustor with the thermoelectric device is out of the scope of the present study. The catalysed monoliths were tested into a lab-microreactor designed to provide a favourable environment for microscale combustion of CH_4/H_2/air lean mixtures to reach high power density (up to $20\,\mathrm{MW_{th}\,m^{-3}}$). In particular, the following catalysts: 2% Pd/(5% $NiCrO_4$), hereafter named Pd/N, 2% Pd/(5% $CeO_2{\cdot}2ZrO_2$), hereafter named Pd/CZ, 2% Pd/(5% $LaMnO_3{\cdot}2ZrO_2$), hereafter named Pd/LZ, and 2% Pt/(5% Al_2O_3), hereafter named Pt/A, were directly deposited on SiC monoliths via in situ Solution Combustion Synthesis (SCS). The carriers' % weights refer to the SiC monolith's weight, and the Pd/Pt % to the carrier's weight.

The catalysts were selected in line with earlier investigations. Pd/N catalysts of various Pd:N ratios were previously studied for micro-combustion of CH_4/H_2/air lean mixtures [35]: the best one was deeply studied in the present work to better understand its performance and used as term of comparison with the other developed catalysts. Pd/CZ catalyst was selected because previously studied as catalysts for CH_4/air combustion [36]; moreover, the CZ system is a very promising catalyst thanks to the good capability of CeO_2 in changing rapidly its oxidation number from Ce^{3+} to Ce^{4+} state, with a consequent O_2 fast release from its lattice to the nearby species [37], helping thus the oxidation phenomena. With the aim to enlarge the knowledge on the catalytic combustion of CH_4/H_2 mixtures, also Pd/LZ catalyst was chosen since previously investigated as catalytic material for CH_4/air combustion [38,39]; moreover, the catalytic activity of perovskite $LaMnO_3$ towards combustion reactions is well known in literature [40–42].

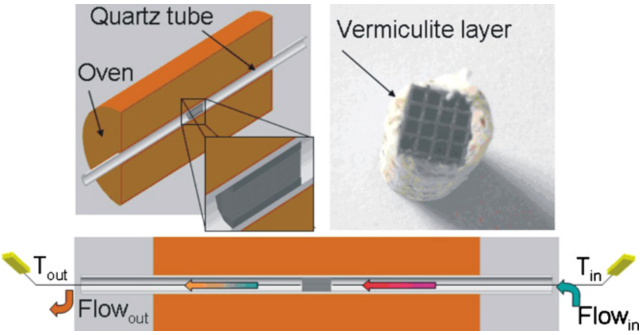

Fig. 1. Sketch of the microreactor placed into the oven and picture of the monolith wrapped by a vermiculite layer.

2. Experimental

The SCS technique was used to prepare the catalysts investigated in the present study. SCS allows the production of advanced porous ceramic or metallic materials, like nanostructured catalysts [38,43]. Homogeneous aqueous solutions containing the metal–nitrate compounds as oxidizers (Aldrich, 99% purity) and urea (for the preparation of $NiCrO_4$ and Al_2O_3) or glycine (for the preparation of $CeO_2{\cdot}ZrO_2$ and $LaMnO_3{\cdot}ZrO_2$) as fuel, dosed in stoichiometric ratio, were used. The ceramic monolith supports made of SiC (6 mm × 6 mm × 22 mm, 16 channels, from CTI, France) were dipped into the solutions and then placed into an oven at 600 °C [35]. The thin solution covering the internal surfaces of the monolith channels was rapidly brought to its boiling point. The main reaction took place, and the desired catalyst was developed onto the surface of the SiC support. The Pd-based monoliths were prepared via one-shot SCS by adding the right amount of $Pd(NO_3)_2$ to the precursors' solutions. The overall deposited Pd amount corresponded to 0.1% of the monolith's weight. Instead, the Pt-based structured catalyst was prepared by first coating with the Al_2O_3 carrier by SCS the internal monolith surfaces, then by adding Pt via drop incipient wetness impregnation starting from a solution of $H_2PtCl_6{\cdot}6H_2O$. The overall deposited Pt amount corresponded to 0.1% of the monolith's weight. Finally, the monoliths were calcined in an oven at 600 °C for about 1 h with still air [35].

The as-prepared monoliths were then characterized by scanning electron microscopy (SEM FEI QUANTA INSPECT LV 30 kV) and field emission scanning electron microscopy (FESEM ZEISS Supra 40), to verify the morphology and the homogeneity of the catalytic layer deposited on the walls of the monolith channels and to check the atomic percentage of the components.

The surface area of all monoliths was determined by N_2 adsorption at the liquid nitrogen temperature using the Micrometrics ASAP 2010M. The surface area was determined according to the Brunauer–Emmett–Teller theory; the samples were degassed in vacuum for at least 4 h at 250 °C before analysis.

The catalytic activity of the as-prepared structured catalysts towards CH_4 combustion, H_2 combustion and CH_4/H_2 lean mixtures combustion was tested in a microreactor test rig [35], as shown in Fig. 1. Each monolith was inserted into a quartz tube (i.d. 10 mm, length 700 mm), wrapped with a vermiculite layer to obtain the external seal; the quartz tube was heated in a horizontal split-tube furnace with 500 mm heating length (Carbolite, PID temperature regulated). For each test, the temperature of the oven was increased from room temperature to 200 °C with a temperature rate of $5\,^{\circ}\mathrm{C\,min^{-1}}$, then from 200 to 800 °C the temperature rate was increased to $10\,^{\circ}\mathrm{C\,min^{-1}}$. Two K-type thermocouples were inserted along the quartz tube, 1 mm upstream and downstream the monolith cross surfaces, to monitor the inlet and outlet temperatures. The reactor outlet–inlet temperature difference was always less

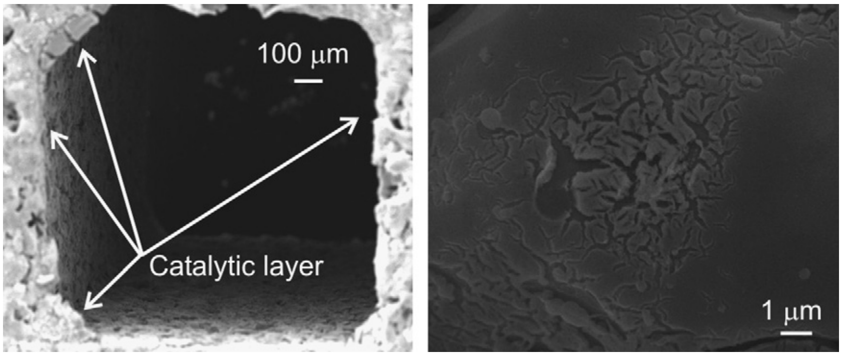

Fig. 2. SEM micrographs of SiC monolith lined with Pd/CZ: microchannel and catalytic layer.

than 10 °C. The monoliths were first tested towards CH_4 combustion by feeding a mixture of 5% vol. CH_4 in air ($\lambda = 2$), overall power density 7.6 $MW_{th}\,m^{-3}$, GHSV of 16,000 h^{-1} based on the monolith empty volume. Then, they were tested towards H_2 combustion by feeding a mixture of 17% vol. H_2 in air ($\lambda = 2$), with the same overall power density and GHSV. Further tests were made on the same monoliths by feeding three different CH_4/H_2 lean mixtures at increased H_2 concentration, maintaining the same values for λ, the overall power density and GHSV: Mix 1 with a CH_4/H_2 molar ratio of 75%/25%; Mix 2 with a CH_4/H_2 molar ratio of 50%/50%; Mix 3 with a CH_4/H_2 molar ratio of 25%/75%. Air, CH_4 and H_2 flowing from cylinders were independently regulated by mass flow controllers (Bronkhorst), premixed, and fed to the microreactor (total flow rate: 200 Nml min^{-1}). The on-line continuous analysis of the gaseous reaction products was performed (after H_2O removal through a condenser) by non-dispersive infrared absorption (NDIR Uras 14 for $CH_4/CO/CO_2$, ABB Company) and a thermal conductivity analyzer (Caldos 17 for H_2, ABB Company), thus allowing to evaluate CH_4 and H_2 conversions. Each test was repeated twice to strengthen the obtained results. The temperatures where 50% conversion of CH_4 or H_2 occurred, CH_4-T_{50} or H_2-T_{50}, respectively, were considered as an index of the monoliths catalytic activity. The homogeneous combustion reactions related to pure CH_4 or H_2 and to the three reactive mixtures were also evaluated by using a bare SiC monolith and also quartz tube reactor without any monolith inside (blank reactor condition); the feeding conditions were the same used during the tests of the catalyzed monoliths.

3. Results and discussion

SEM and FESEM analysis of the as-prepared monoliths highlighted a quite porous catalyst layer onto the internal walls of the monoliths channels. Figs. 2 and 3 show SEM images of monoliths Pd/CZ and Pd/N, respectively; Figs. 4 and 5 show FESEM images of the catalytic layer on monoliths Pd/LZ and Pt/A, respectively. Such a porous structure, particularly evident on samples Pd/LZ (also at nanometric scale) and Pd/N, is typical when SCS technique is adopted for catalytic material development [35,38,43]. During SCS, in fact, the decomposition of reacting precursors generated a large amount of gaseous products in a very short time, leading thus to a spongy morphology of the synthesized layer [38,43]. The average thickness of the catalytic layer varied from approx 10 to 50 μm, with a preferential accumulation on the channels corners, especially for the Pd/N and Pd/CZ monoliths. FESEM analysis (Figs. 4 and 5), allowed to better emphasize the structure of the catalytic layer: in particular, on Pt/A monolith, Pt clusters homogeneously distributed alongside the carrier were visible, with dimensions variable from 10 to 100 nm.

The catalyst deposition over the bare monoliths induced an increase of the BET specific surface areas, as expected. The calculated BET values were 2.9 $m^2\,g^{-1}$ for Pd/N monolith, 12.2 $m^2\,g^{-1}$ for Pd/CZ, 13.7 $m^2\,g^{-1}$ for Pd/LZ and 14.5 $m^2\,g^{-1}$ for Pt/A one, respectively, compared to the 0.2 $m^2\,g^{-1}$ of the bare monolith.

The first step to evaluate the catalytic activity of the as-prepared monoliths was carried out in the lab test rig, feeding only CH_4 in lean mixture; the performance of the various catalysed monoliths was compared with that of the bare one. As reported in Fig. 6, the Pt/A monolith showed the best performance, lowering the CH_4-T_{50} from 777 to 617 °C and the CH_4-T_{100}, from 780 to 716 °C, compared to the bare monolith counterpart (SiC). The CH_4-T_{100} of all the Pd-based catalyzed monoliths resulted slightly higher compared to the the base SiC monolith. Followed Pd/CZ with CH_4-T_{50} of 650 °C, Pd/N with CH_4-T_{50} of 678 °C and Pd/LZ with CH_4-T_{50} of 743 °C. Moreover, as concerns the CO emissions (Fig. 6, dotted lines) during CH_4 combustion tests, the bare monoliths presented a very high peak between CH_4-T_{90} and CH_4-T_{100} (approx 2.4% in volume). Instead, all the catalytic monoliths were able to lower this peak concentration with the following rank: in particular, Pt/A and Pd/CZ exhibited very low CO emissions (approx 100 and 300 ppmv, respectively),

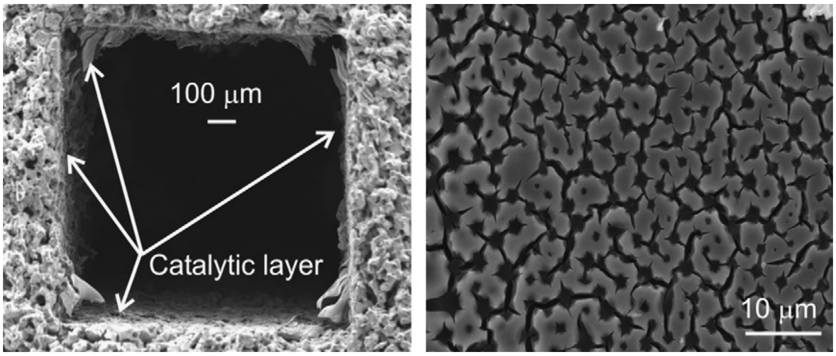

Fig. 3. SEM micrographs of SiC monolith lined with Pd/N: microchannel and catalytic layer.

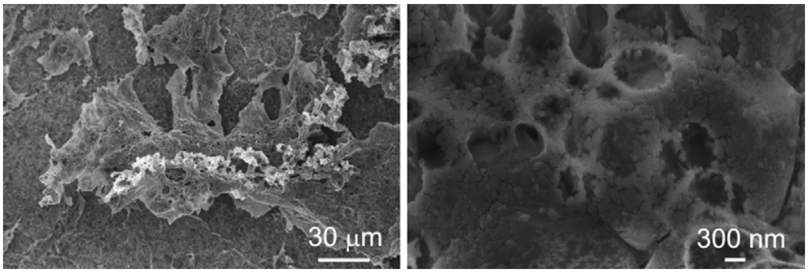

Fig. 4. FESEM micrographs of the catalytic layer on Pd/LZ monolith.

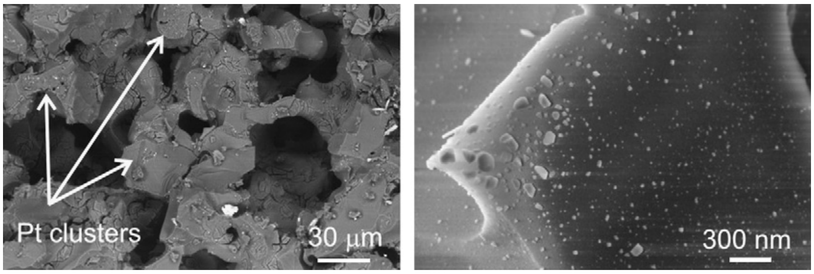

Fig. 5. FESEM micrographs of the catalytic layer on Pt/A monolith: Pt particles are enlightened.

whereas Pd/N presented a limited peak (approx 900 ppmv) and Pd/LZ, which showed the worse performance towards CH_4 combustion, presented a quite high peak (approx 1.1%), when CH_4 was almost reacted.

The second step regarded the evaluation of the catalytic activity of the as-prepared monoliths towards H_2 combustion in lean mixture. The results are reported in Fig. 7: all the catalytic monoliths were able to sensibly reduce the H_2 combustion temperature compared to the one in the bare monolith (H_2-T_{50}: 660 °C; H_2-T_{100}: 690 °C). In particular, Pt/A was the best one: practically at room temperature H_2 was completely burnt (H_2-T_{50}: 39 °C; H_2-T_{100}: 40 °C). The other monoliths behave as follow: Pt/A < Pd/N (H_2-T_{50}: 141 °C; H_2-T_{100}: 160 °C) < Pd/CZ (H_2-T_{50}: 177 °C; H_2-T_{100}: 204 °C) < Pd/LZ (H_2-T_{50}: 201 °C; H_2-T_{100}: 216 °C).

Thanks to these very interesting performances, all the catalyzed monoliths were used for further investigations on combustion of CH_4/H_2 lean mixtures. A comparison of the CH_4 and H_2 conversion curves vs. *T* for all the catalysed monoliths, the bare one included, is shown in Fig. 8, where the curves are displayed per tested Mix (Fig. 8A for Mix 1 – CH_4/H_2 molar ratio of 75/25; Fig. 8B for Mix 2 – CH_4/H_2 molar ratio of 50/50; Fig. 8C for Mix 3 – CH_4/H_2 molar ratio of 25/75). Fig. 9, instead, shows the same conversion curves displayed per tested monolith (Fig. 9A for Pd/N; Fig. 9B for Pd/CZ; Fig. 9C for Pd/LZ; Fig. 9D for Pt/A).

On average, by observing Fig. 8, it is worth noting that the presence of a catalyst on the SiC monolith allowed reducing the CH_4-T_{50} and CH_4-T_{100} compared to the bare counterpart, for all the tested Mix. Moreover, the higher the H_2 concentration, the lower the CH_4-T_{50} (see Fig. 8C with Mix 3): the addition of H_2 in the reactive mixture seemed to favour the CH_4 combustion. Considering the homogeneous CH_4 combustion reaction occurring when the various mixtures were tested, the performances obtained with the bare monolith and the blank reactor (no monolith inside) were practically the same (curves denoted with solid black lines and the letter “a” in Fig. 8A/B/C). It is worth noting that an H_2 enrichment was favourable to CH_4 combustion also without the presence of a catalytic layer on the monolith walls: the related CH_4-T_{50} and CH_4-T_{100} were, in fact, slightly decreased by increasing the H_2 concentration in the feedstock (CH_4-T_{50} Mix 1/2/3: 777/736/718 °C; CH_4-T_{100} Mix 1/2/3: 800/790/780 °C). This seems to be a clear sigh that there was a contribution of the homogeneous reaction in the combustion of CH_4 when H_2 was added as fuel. Concerning the CO emissions, these

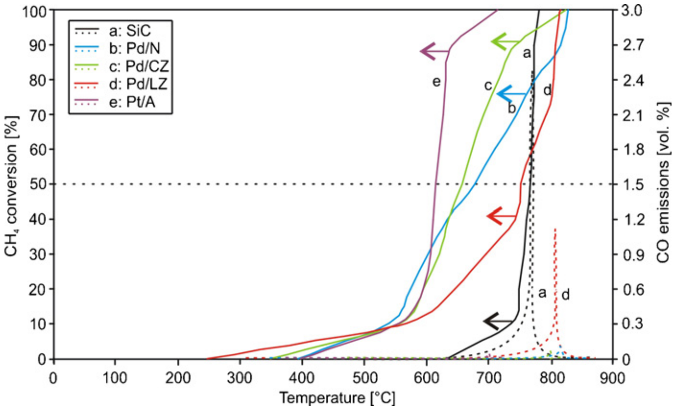

Fig. 6. CH_4 conversion (solid lines) and CO emissions (dotted lines) vs. *T* for the as-prepared catalytic monoliths and the bare one (a: SiC; b: Pd/N; c: Pd/CZ; d: Pd/LZ; e: Pt/A).

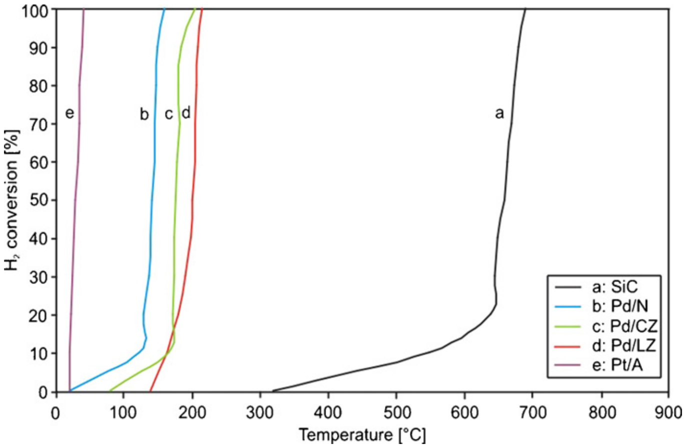

Fig. 7. H_2 conversion vs. *T* for the as-prepared catalytic monoliths and the bare one (a: SiC; b: Pd/N; c: Pd/CZ; d: Pd/LZ; e: Pt/A).

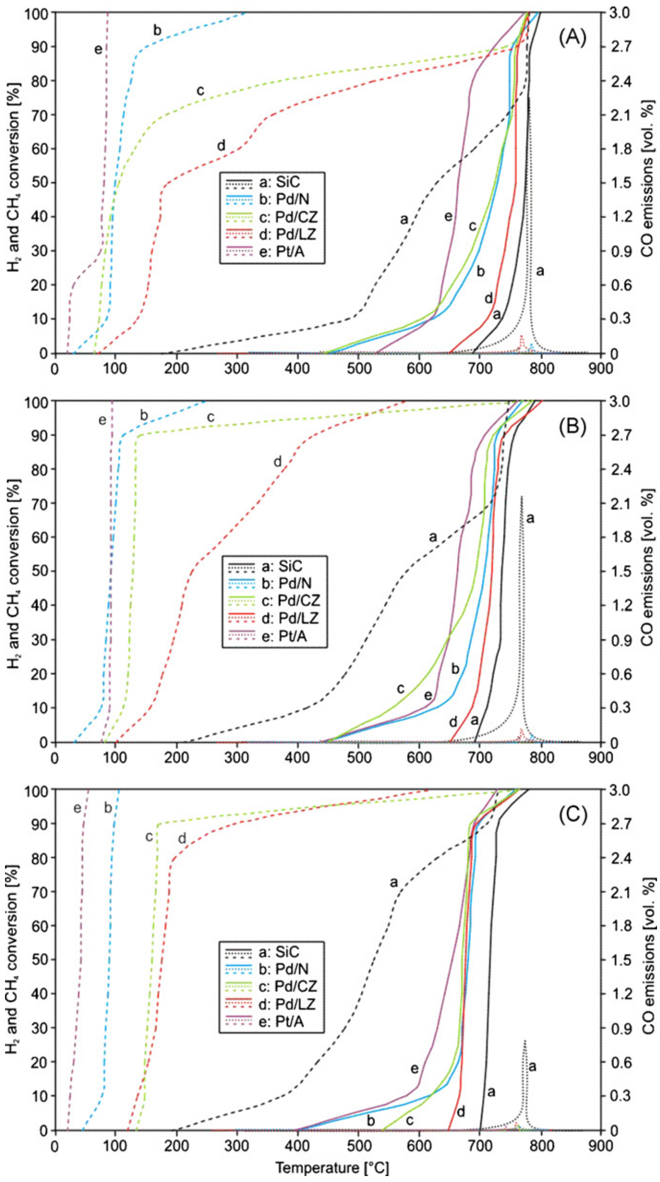

Fig. 8. CH_4 conversion (solid lines), H_2 conversion (broken lines) and CO emissions (dotted lines) vs. *T* for the three gas mixtures (A: Mix 1 CH_4/H_2 molar ratio 75/25; B: Mix 2 CH_4/H_2 molar ratio 50/50; C: Mix 3 CH_4/H_2 molar ratio 25/75) on all the tested monoliths (a: SiC; b: Pd/N; c: Pd/CZ; d: Pd/LZ; e: Pt/A).

were quite high for the bare monolith, anyway lower compared to the test with CH_4 alone and decreasing by increasing the H_2 concentration in the mixtures: 2.31% for Mix 1, 2.23% for Mix 2, 0.78% for Mix 3, respectively, see Fig. 8. The CO emissions of the catalytic monoliths, lower compared to the test with CH_4 alone, were still reduced by increasing the H_2 concentration in the mixture, with the same trend observed for the bare monolith; the highest CO emission peak, 0.21%, belonged to Pd/LZ when tested with Mix 1, see Fig. 8A, whereas the peak concentrations were below 50 ppmv for the Pt/A monolith.

Indeed, considering the H_2 combustion in the tested Mix 1/2/3, the performance of the monoliths was different. Compared to the bare one, all the catalytic monoliths reduced the H_2-T_{50}, whereas the H_2-T_{100} was practically decreased only for monoliths Pt/A and Pd/N (see also Fig. 9A and D). In particular, for Mix 1 and Mix 2, i.e., when the H_2 concentration in the mixture was lower or lower than that of CH_4 (Fig. 8A and B), the H_2 combustion started at very low temperature (very low H_2-T_{10} and H_2-T_{50}, a sign of good reactivity),

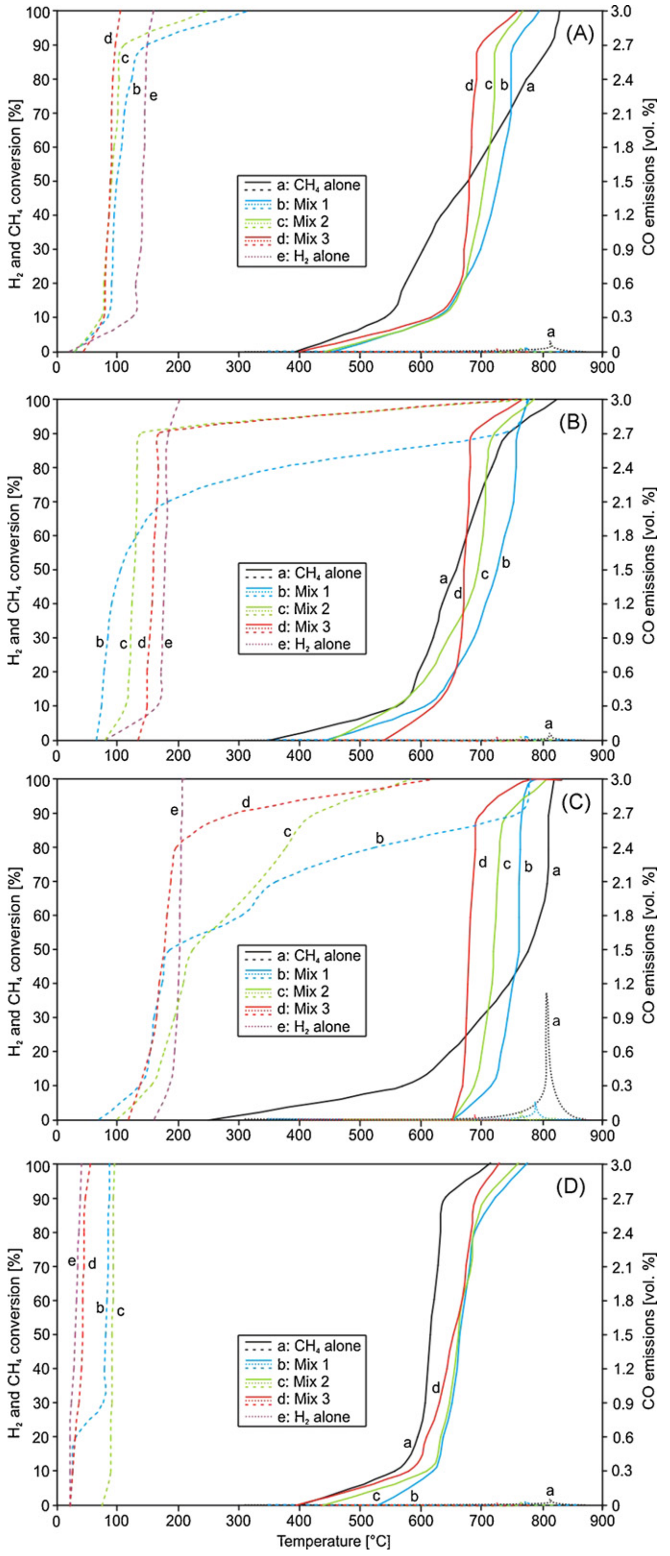

Fig. 9. CH_4 conversion (solid lines), H_2 conversion (broken lines) and CO emissions (dotted lines) vs. *T* for each catalytic monolith (A: Pd/N; B: Pd/CZ; C: Pd/LZ; D: Pt/A) as a function of the fed reactive mixture (a: CH_4 alone; b: Mix 1 CH_4/H_2 molar ratio 75/25; c: Mix 2 CH_4/H_2 molar ratio 50/50; d: Mix 3 CH_4/H_2 molar ratio 25/75; e: H_2 alone).

but the combustion rate was slowed down during the tests: the conversion curves slope became, in fact, less steep and the H_2-T_{100} of Mix 1 and 2 raised compared to the H_2-T_{100} of pure H_2. Especially for Pd/CZ and Pd/LZ (Fig. 9B and C), the H_2-T_{100} raised up to the same value of the CH_4-T_{100}.

The combustion in confined space where lots of walls are present is mainly affected by quenching and blowout [33]. Flames are quenched because of two primary mechanisms, namely thermal and radical quenching [44–46]. Thermal quenching occurs when sufficient heat is removed through the walls, the combustion, thus, cannot be self-sustained. Radical quenching occurs via adsorption of radicals on the burner walls and subsequent recombination. In case of H_2/air mixtures, $OH^\bullet$, $H^\bullet$ and $HO_2{}^\bullet$ radicals are present [47]: the most relevant reactions in the formation/destruction of these radicals are the chain radical formation, the chain radical propagation, the chain radical ramification and the chain radical termination. These latter, leading to the formation of stable species, can occur via homogeneous or heterogeneous process (when they impact the burner walls) [47]. In case of CH_4/air mixtures, $OH^\bullet$ radicals play the most relevant role in the combustion light-off in the gas phase: these radicals, in fact, chemically activate the CH_4 molecules by abstracting $H^\bullet$ radicals from them, thus producing $CH_3{}^\bullet$ via the reaction: $CH_4 + OH^\bullet \rightarrow CH_3{}^\bullet + H_2O$ [47]. By adding H_2 to CH_4, a changing in the $OH^\bullet$ formation mechanism occurs: in particular, by increasing H_2, $OH^\bullet$ radicals are produced more and more significantly through the reaction $HO_2{}^\bullet + H^\bullet \rightarrow 2OH^\bullet$, which starts from $HO_2{}^\bullet$ radical, an intermediate product of low temperature H_2 combustion [47]. Such a reaction is also known in literature to give a higher $OH^\bullet$ concentration in the early flame [48]. More specifically, the presence of H_2 in the fuel improves system performances in converting CH_4, because determines an increase in the production of $OH^\bullet$ radicals at a temperature relatively low thus allowing HC combustion in the gas phase at a lower thermal level [47]. The increased $OH^\bullet$ concentration when H_2 is added to CH_4 was experimentally demonstrated also on a swirl flame [49].

In addition to flame quenching, blowout can occur when the burner exit velocity exceeds the flame burning velocity [46]. In this mechanism, the reaction shifts downstream until it exits the micro-burner. A stable flame in micro-burners can be achieved through appropriate surface modification to limit radical loss, i.e., through catalyst deposition (a catalytic layer could help the combustion process at the micro-burner walls, which are well-knows to influence the formation of reactive radicals), and increasing insulation to limit heat losses.

Under the investigated conditions, the observed increase in reactivity of the mixture when CH_4 was enriched with H_2, independent of the type of catalyst lined on the monolith, could be explained by an increase in the $OH^\bullet$ reactive radicals. Moreover, CH_4/H_2 mixtures burned also in the gas phase, thanks to the contribution of the homogeneous combustion reactions. Surely, the catalysts remain certainly determinant in oxidizing CO to CO_2 improving thus the combustion efficiency.

4. Conclusions

The combustion of gaseous HC fuels in a small confined space could represent an alternative way to produce thermal and electrical energy. The combustion of CH_4 and its lean mixtures with H_2 on catalytic monoliths was studied and optimized. 2% Pd/(5% $NiCrO_4$), 2% Pd/(5% $CeO_2{\cdot}ZrO_2$), 2% Pd/(5% $LaMnO_3{\cdot}ZrO_2$) and 2% Pt/(5% Al_2O_3) catalysts, suitably developed, were deposited on SiC monoliths via in situ SCS and tested in a lab-scale microreactor by feeding only CH_4, only H_2, and three lean CH_4/H_2 mixtures with increased content of H_2 and constant thermal power density of 7.6 $MW_{th}\ m^{-3}$. Monolith Pt/A was very appropriate for the combustion of only CH_4 or H_2, but its performance worsen when H_2 was added to the reactive mixture. On the contrary, the Pd-based catalysts were most suitable for the combustion of the CH_4/H_2 lean mixtures, with the best behaviour shown by Pd/N followed by Pd/CZ. Monolith Pd/LZ, instead, showed the worse performance, both in terms of CH_4 combustion only and of the various mixtures; moreover, it displayed quite high CO emissions, not compatible with the environmental issues. In particular, the catalytic reactivity towards CH_4 combustion of the Pd-based raised by increasing the H_2 content in the reactive mixture. The observed enhancement in reactivity of the mixture when the CH_4 fuel was enriched with H_2 could be explained by an increase of the $OH^\bullet$ radicals in the gas mixture.

References

[1] M.F.M. Zwinkels, S.G. Järås, P.G. Menon, T.A. Griffin, Catal. Rev. Sci. Eng. 35 (1993) 319.
[2] H. Arai, M. Machida, Appl. Catal. A: Gen. 138 (1996) 161.
[3] P. Forzatti, G. Groppi, Catal. Today 54 (1999) 165.
[4] J.J. Spivey, Ind. Eng. Chem. Res. 26 (1987) 2165.
[5] R. Kikuchi, Y. Tanaka, K. Sasaki, K. Eguchi, Catal. Today 83 (2003) 223.
[6] D.L. Trimm, Appl. Catal. 7 (1983) 249.
[7] R.F. Hicks, H. Qi, M.L. Young, R.G. Lee, J. Catal. 122 (1990) 280.
[8] G. Corro, J.L.G. Fierro, O. Vazquez, Catal. Commun. 6 (2005) 287.
[9] O. Demoulin, B. Le Clef, M. Navez, P. Ruiz, Appl. Catal. A: Gen. 334 (2008) 1.
[10] O. Deutschmann, L. Maier, U. Ridel, A. Stroemman, R. Dibble, Catal. Today 59 (2000) 141.
[11] http://www.hythane.com.
[12] S.O. Akansu, Z. Dulger, N. Kahraman, T.N. Veziroglu, Int. J. Hydrogen Energy 29 (2004) 1527.
[13] F. Ortenzi, M.C., R. Scarcelli, G. Pede, Int. J. Hydrogen Energy 33 (2008) 3225.
[14] http://www.mobiliter.eu.
[15] http://www.greenfuelforecast.com.
[16] http://www.managenergy.net.
[17] C.J. Tseng, Int. J. Hydrogen Energy 27 (2002) 699.
[18] W.M. Yang, S.K. Chou, C. Shu, H. Xue, Z.W. Li, D.T., J.F. Pan, Energy Convers. Manage. 44 (2003) 2625.
[19] Y. Zhang, J. Zhou, W. Yang, M. Liu, K. Cen, Int. J. Hydrogen Energy 32 (2007) 1286.
[20] Y. Wang, Z. Zhou, W. Yang, J. Zhou, J. Liu, Z. Wang, K. Cen, Energy Convers. Manage., in press, doi:10.1016/j.enconman.2009.12.021.
[21] M. Iamarino, P. Salatino, R. Chirone, R. Pirone, G. Russo, Proc. Comb. Inst. 29 (2002) 827.
[22] J. Lee, D. Trimm, Fuel Process Technol. 42 (1995) 339.
[23] R.A. Dalla Betta, Catal. Today 35 (1997) 129.
[24] P. Gélin, M. Primet, Appl. Catal. B: Environ. 39 (2002) 1.
[25] O. Demoulin, M. Navez, E.M. Gaigneaux, P. Ruiz, A.-S. Mamede, P. Granger, E. Payen, Phys. Chem. Chem. Phys. 5 (2003) 4394.
[26] R. Burch, P.K. Loader, Appl. Catal. B: Environ. 5 (1994) 149.
[27] M. Alifanti, J. Kirchnerova, B. Delmon, D. Klvana, Appl. Catal. A: Gen. 262 (2004) 167.
[28] A.C. Fernandez-Pello, Proc. Combust. Inst. 29 (2003) 883.
[29] M. Shannon, R.I. Miesse, M. Masel, Combust. Theory Modell. 9 (2005) 77.
[30] J. Vican, B.F. Gajdeczko, F.L. Dryer, D.L. Milius, I.A. Aksay, R.A. Yetter, Proc. Combust. Inst. 29 (2002) 909.
[31] J.A. Federici, D.G. Norton, T. Bruggemann, K.W. Voit, E.D. Wetzel, D.G. Vlachos, J. Power Sources 161 (2006) 1469.
[32] C.M. Miesse, R.I. Masel, C.D. Jensen, M.A. Shannon, M. Short, AIChE J. 50 (2004) 3206.
[33] D.G. Norton, D.G. Vlachos, Chem. Eng. Sci. 58 (2003) 4871.
[34] N.S. Kaisare, D.G. Vlachos, Catal. Today 120 (2007) 96.
[35] S. Specchia, L.D. Vella, S. Burelli, G. Saracco, V. Specchia, Chem. Phys. Phys. Chem. 10 (2009) 783.
[36] S. Specchia, E. Finocchio, G. Busca, G. Saracco, V. Specchia, Catal. Today 143 (2009) 86.
[37] M. Boaro, M. Vicario, C. de Leitenburg, G. Dolcetti, A. Trovarelli, Catal. Today 77 (2003) 407.
[38] S. Specchia, A. Civera, G. Saracco, Chem. Eng. Sci. 59 (2004) 5091.
[39] S. Specchia, P. Palmisano, E. Finocchio, M.A. Larrubia Vargas, G. Busca, Appl. Catal. B: Envion. 92 (2009) 285.
[40] T. Seyama, Catal. Rev. Sci. Eng. 34 (1992) 281.
[41] R. Spinicci, A. Delmastro, S. Ronchetti, A. Tofanari, Mater. Chem. Phys. 78 (2003) 393.
[42] A. Civera, G. Negro, S. Specchia, G. Saracco, V. Specchia, Catal. Today 100 (2005) 275.
[43] K.C. Patil, S.T. Aruna, T. Mimani, Curr. Opin. Solid State Mater. Sci. 6 (2002) 507.
[44] D.G. Vlachos, L.D. Schmidt, R. Aris, Combust. Flame 95 (1993) 313.
[45] D.G. Vlachos, L.D. Schmidt, R. Aris, AIChE J. 40 (1994) 1005.
[46] J. Daou, Combust. Flame 128 (2002) 321.
[47] P. Dagaut, A. Nicolle, Proc. Combust. Inst. 30 (2005) 2631.
[48] S.S. Shy, Y.C. Chen, C.H. Yang, C.C. Liu, C.M. Huang, Combust. Flame 153 (2008) 510.
[49] R. Schefer, Int. J. Hydrogen Energy 28 (2003) 1131.